Journal of Pharmaceutical and Biomedical Analysis 158 (2018) 236–246

Contents lists available at ScienceDirect

Journal of Pharmaceutical and Biomedical Analysis

journal homepage: www.elsevier.com/locate/jpba

Multiwavelength UV-metric and pH-metric determination of the multiple dissociation constants of the lesinurad

Milan Meloun[a,*], Aneta Čápová[a], Lucie Pilařová[a], Tomáš Pekárek[b]

[a] Department of Analytical Chemistry, University of Pardubice, CZ 532 10 Pardubice, Czech Republic
[b] Zentiva k.s., U kabelovny 130, CZ 102 37 Prague, Czech Republic

ARTICLE INFO

Article history:
Received 14 March 2018
Received in revised form 23 May 2018
Accepted 29 May 2018
Available online 4 June 2018

Keywords:
Dissociation constants
Lesinurad
Spectrophotometric titration
pH-titration
REACTLAB
SQUAD84
ESAB

ABSTRACT

Potentiometric and spectrophotometric pH-titrations of the lesinurad for three consecutive dissociation constants determination were compared. Lesinurad is a selective inhibitor of uric acid reabsorption as part of a combination of medicines to treat high levels of uric acid in blood, also called hyperuricemia. Nonlinear regression of the pH-spectra with REACTLAB and SQUAD84 and of the pH-titration curve with ESAB determined three multiple close dissociation constants. The protonation scheme of lesinurad was suggested. A sparingly soluble anion L^- of lesinurad was protonated to the still soluble species LH, LH_2^+ and LH_3^{2+} in pure water. Three consecutive thermodynamic dissociation constants were estimated $pK^T_{a1} = 2.09$, $pK^T_{a2} = 4.25$, $pK^T_{a3} = 6.58$ at 25 °C and $pK^T_{a1} = 1.96$, $pK^T_{a2} = 4.16$, $pK^T_{a3} = 6.32$ at 37 °C by UV-metric spectra analysis. The graph of molar absorption coefficients shows that the spectrum of species LH_2^+ and LH vary in colour, while protonation of chromophore LH_2^+ to LH_3^{2+} has less influence on chromophores in the lesinurad molecule. Three multiple thermodynamic dissociation constants of 1×10^{-4} M lesinurad were determined by the pH-metric analysis $pK^T_{a1} = 2.39$, $pK^T_{a2} = 3.47$, $pK^T_{a3} = 6.17$ at 25 °C and $pK^T_{a1} = 2.08$, $pK^T_{a2} = 3.29$, $pK^T_{a3} = 6.03$ at 37 °C. The values of enthalpy $\Delta H^0(pK_{a1}) = 19.19\ kJ\ mol^{-1}$, $\Delta H^0(pK_{a2}) = 13.29\ kJ\ mol^{-1}$, $\Delta H^0(pK_{a3}) = 38.39\ kJ\ mol^{-1}$, show the dissociation process is endothermic. The positive values of $\Delta G^0(pK_{a1}) = 11.93\ kJ\ mol^{-1}$, $\Delta G^0(pK_{a2}) = 24.26\ kJ\ mol^{-1}$, $\Delta G^0(pK_{a3}) = 37.56\ kJ\ mol^{-1}$ at 25 °C indicate that the dissociation process of pK_{a2} is not spontaneous, which was confirmed by its value of entropy $\Delta S^0(pK_{a1}) = 24.37\ J\ mol^{-1}$, $\Delta S^0(pK_{a2}) = -36.79\ J\ mol^{-1}$, $\Delta S^0(pK_{a3}) = 2.79\ J\ mol^{-1}$. Three macro-dissociation constants of lesinurad and protonation locations were predicted by MARVIN and ACD/Percepta.

1. Introduction

Lesinurad is the urate transporter inhibitor for treating hyperuricemia associated with gout. The IUPAC chemical designation of lesinurad is 2–((5-bromo-4-(4-cyclopropylnaphthalen-1-yl)–4H-1,2,4- triazol-3–yl)thio)acetic acid with the molecular formula $C_{17}H_{14}BrN_3O_2S$ and there are various chemical names for lesinurad such as 878672-00-5; RDEA594; Zurampic; RDEA 594; UNII-09ERP08I3W. The molecular weight is 404.28 g/mol and water solubility is 0.00779 mg/mL. The registration number is CAS 878672-00-5 and PubChem CID 53465279, UNII 09ERP08I3W. Lesinurad has the trademark Zurampic (Fig. 1).

Gout is the most common inflammatory arthritis disseminated throughout the world [1]. Gout is caused by an increased level of the serum uric acid. It is three to four times more common in males than in women, and prevalence increases with age [2]. Increased concentrations of uric acid in the body result in the deposition of monosodium urate crystals, especially in joints. These crystals trigger the release of pro-inflammatory cytokines, especially interleukin(IL)-1-beta, which stimulates inflammation, and this results in great joint sensitivity and pain [3]. The acute stage is treated with short-term anti-inflammatory drugs, but long-term prevention can be achieved by lowering serum uric acid levels. Current urate-lowering drugs include both xanthine oxidase inhibitors and uricosuric agents. Recent advances in the role of urate transporters in kidney proximal tubules have resulted in the development of new generation uricosuric drugs including lesinurad [4]. Lesinurad belongs to the class of organic compounds known as phenyl-1,2,4-triazoles. It is a selective inhibitor of uric acid reabsorption which is used in combination with other agents in treating gout. It reduces serum uric acid concentration through the inhibition of an oral uric acid transporter 1 (URAT1) inhibitor, an enzyme

* Corresponding author.
E-mail address: milan.meloun@upce.cz (M. Meloun).

https://doi.org/10.1016/j.jpba.2018.05.047
0731-7085/

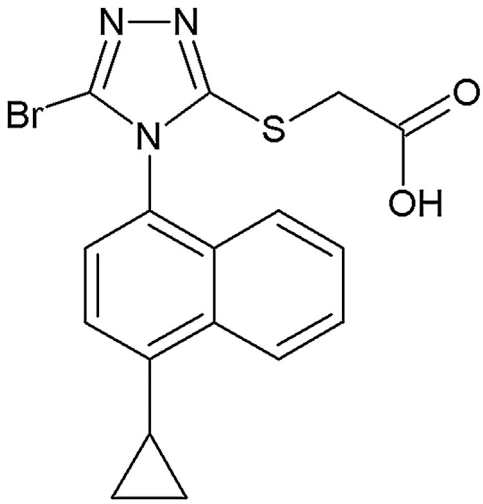

Fig. 1. Structural formula of lesinurad.

responsible for the reuptake of uric acid from the renal tubule, and OAT4, another uric acid transporter associated with diuretic-induced hyperuricemia. Lesinurad helps the kidneys remove uric acid from the body. Lesinurad 200 mg daily in combination with a xanthine oxidase is approved for urate-lowering therapy in patients with gout. Lesinurad combined with the xanthine oxidase inhibitor (XO) provides an effective treatment for gout-related hyperuricaemia. It was approved on December 2015 by the US Food and Drug Administration (FDA) and by the European Medicines Agency (EMA) in February 2016, ref. [5].

One of the most important physico-chemical characteristics of every drug is considered its pK_a value, which is a key physicochemical parameter influencing many biopharmaceutical characteristics in pharmacokinetic and bioavailability studies [6–9]. The dissociation constants of a compound influences lipophilicity, solubility, and permeability and plays a crucial role in the characterization of its absorption, distribution, metabolism and excretion (ADME) profile [10–14]. pK_a values can be either experimentally measured or theoretically predicted:

1. Spectrophotometry, and UV-metric spectra analysis (also called WApH technique [15]) in particular, is a highly sensitive convenient method to determine pK_a in very diluted aqueous solutions since it requires relatively simple equipment and can work with a sub-micromolar compound concentration (about 10^{-5} to 10^{-6} M), *cf. ref.*[16–18]. The authors [19–22] have shown that spectrophotometric titration in combination with suitable chemometric tools can be used to determine dissociation constants pK_a even for sparingly soluble drugs [20] [23]. The most relevant algorithms are SQUAD84 [17] and REACTLAB [24]. It is still believed that spectrophotometric data are inherently less precise than potentiometric data [25]; consequently most equilibrium constants are determined by means of pH-metric potentiometric titrations using ESAB [26] or HYPERQUAD [27,28].
2. The accuracy of theoretical pK_a predictions from a molecular structure with two predictive programs ACD/Percepta [29–35], MARVIN [29,31,32,34,36–39] was found to be the best of all nine similar programs.

The aim of our study was to examine the regression analysis of the pH-absorbance matrix with very small changes in spectra and to carry out a pH-metric potentiometric determination of the protonation model to find suitable conditions for a reliable regression determination of dissociation constants.

2. Computational details

Spectrophotometric pH-titration data were treated using the program SQUAD84 [17] and REACTLAB [24] which calculates equilibrium (protonation or dissociation) constants and molar absorptivities spectral profiles and distribution diagram of the relative concentrations of the pure species by the nonlinear regression of pH-spectra. A detailed tutorial of tittration also called the WApH technique [15], and alternative pH-metric titration have been was previously described [20,23].

3. Materials and methods

3.1. Materials

Lesinurad donated by ZENTIVA k. s., (Prague) with declared purity checked by a HPLC method and alkalimetrically, was always >99%. This drug was weighted straight to a reaction vessel resulting in a concentration of about 9.9×10^{-5} M. Other chemicals have been previously described [20].

3.2. Apparatus

The apparatus used and both titration procedures were described in detail [21–23,40]. The experimental and computation scheme to determine the dissociation constants of the multicomponent system is taken from Meloun et al., cf. page 226 in ref. [41] and all steps are described in details [21]. The free hydrogen-ion concentration [H^+] was measured on the digital voltmeter Hanna HI 3220 with a precision of ±0.002 pH using the combined glass electrode Theta HC 103-VFR. The potentiometric titrations of drugs with potassium hydroxide were performed using a hydrogen activity scale. Standardization of the pH meter was performed using WTW standard buffers values, 4.006 (4.024), 6.865 (6.841) and 9.180 (9.088) at 25 °C and 37 °C, respectively, in brackets.

3.3. Software

An estimation of the dissociation constants was performed by the nonlinear regression analysis of the UV-metric spectra analysis using SQUAD84 [17], REACTLAB [24] programs and potentiometric pH-metric titration data using the ESAB program [26,42], and by spectra interpretation using the INDICES program [43]. Most graphs were plotted using ORIGIN 9.1, ref [44]. ACD/Percepta [29–35] and MARVIN [29,31,32,34,36–39] programs for predictions of pK_a's are based on the structural formulae of drug compounds.

4. Results

The methods of analysis of the pH-absorbance response and pH-potentiometric titration curves have proven to be the best instrumental methods reliably determine close consecutive dissociation constants of even sparingly soluble drugs. Spectroscopic titration has been utilized as an alternative to potentiometric method to determine pK_a values of substances with large molar absorptivities due to its high sensitivity to concentrations of substance as low as 10^{-5} M. However, the examined compound must posses chromophore(s) in proximity to the ionization center(s) so that the protonated and deprotonated species exhibit sufficient spectral dissimilarity. The nonlinear regression analysis of spectrophotometric data is an effective and reliable tool, even in a case of small changes in spectra when changing the pH of the chromophore.

4.1. UV-metric spectra analysis

The experimental procedure and computational strategy for determining the dissociation constants by analysing the pH-absorbance matrix has been described in our published Tutorial [21]. In addition to determining the number of protonation equilibria, the number of differently protonated species, the diagram of their relative concentration and the graph of their molar absorption coefficients at wavelengths range, the criteria of reliability of the found protonation model should also be stated. The first step of this analysis is the prediction of dissociation constants, based on a quantum-chemical calculation, concerned the structural pattern of the studied molecule.

Step 1: *Prediction of pK_a estimates from the lesinurad structure:* The predictive program MARVIN indicated three protonizable sites of lesinurad A, B, C, which can be associated with three dissociation constants. The two protonation centers A and B are located on nitrogen atoms and the third position C refers to the carboxyl group. The electronic nature of the nitrogen atoms in the molecule varies considerably because it is influenced by various electronic and steric effects. To facilitate the prediction of dissociation constants, the lesinurad molecule was subdivided into three suitable fragments in Fig. 2. These fragments represent similar molecules that could be considered as simplified portions of lesinurad with the protonation centers A, B and C. For example, the protonation center A in fragments exhibits pK close to the pK of lesinurad molecule. A similar conclusion also was found for the protonation center of carboxyl group C. At the protonation center B, however, there is a variation in the estimation of pK fragments in comparison to lesinurad. The ACD/Percepta program displays similar predicted values pK as is achieved with the MARVIN program.

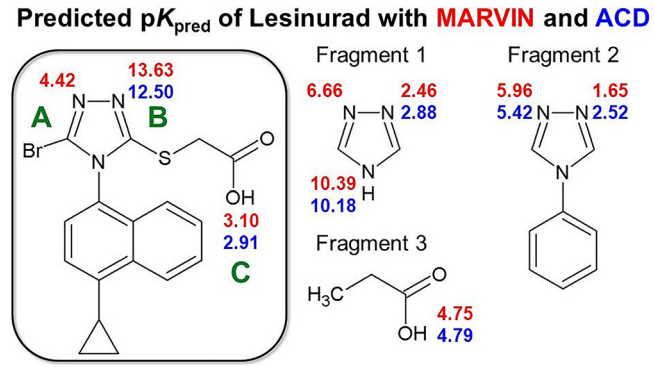

Fig. 2. Molecular structure of lesinurad (inset) with highlighted basic centers A, B and C and predicted pK_a values using MARVIN/ACD prediction programs. Structure of auxiliary fragments 1–3 and their predicted pK_a.

Step 2: *Number of light-absorbing species n_c:* Lesinurad contains a complicated molecular structure introduced in Figs. 1 and 2 and several protonation equilibria can be monitored spectrophotometrically. The spectral data set in the form of the absorbance-response-matrix **A** obtained at various pH values was subjected to factor analysis to determine the number of independent light-absorbing species, n_c. It was carried out with the use of the absorbance matrix rank calculated in the INDICES algorithm [43]. The absorbance matrix **A** contains m columns of the measured pH values and n wavelength lines. INDICES algorithm [43] draws a graph $s_k(A)$ relative to index k (Fig. 3). The found solution is k^*, which is a coordinate of the significant break on the curve $s_k(A) = f(k)$. There are many modifications to this approach from var-

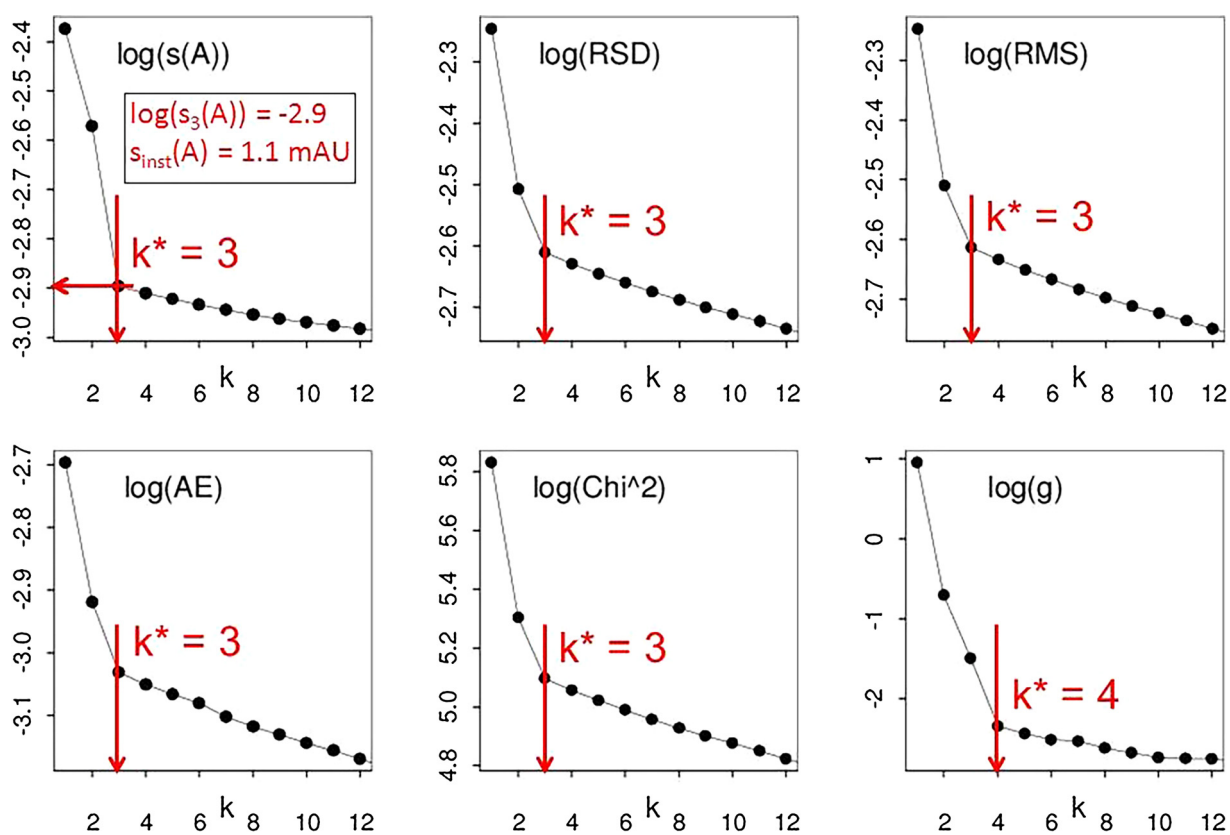

Fig. 3. Five modifications of the Cattel's scree plot log $s_k(SV) = f(k)$ of the of singular value decomposition SVD for the rank estimation of the absorbance matrix (the residual standard deviation RSD, the root mean error square RMS, the average error criterion AE, χ^2 criterion Chi2) lead to $k^* = 3$ in logarithmic scale for lesinurad. $n_c = 3$, and one modification (the standard deviation of eigenvalues g_k) lead to $k^* = 4$, (INDICES in S-PLUS), [42].

Table 1
The regression refinement of three dissociation constants pK_{a1}, pK_{a2}, pK_{a3} of lesinurad with SQUAD84 and REACTLAB at 25 °C and 37 °C in dependence on the ionic strength. Solution of 9.9×10^{-5} M lesinurad for n_s spectra measured at n_w wavelengths for $n_z = 2$ basic components L and H forms variously protonated species. The standard deviations of the parameter estimates are in the last valid digits in brackets. The resolution criterion and reliability of parameter estimates found were proven with goodness-of-fit statistics such as the residual standard deviation by factor analysis $s_k(A)$ [mAU] the mean residual $E|\bar{e}|$ [mAU] the standard deviation of absorbance after termination of the regression process $s(\hat{e})$ [mAU] the sigma $s(A)$ [mAU] from REACTLAB and the Hamilton R-factor of relative fitness [%] from SQUAD84.

Temperature		25 °C					37 °C				
Ionic strength [mol/L]		0.0329	0.0399	0.0478	0.0624	0.0769	0.0178	0.0329	0.0478	0.0624	0.0769
Cattel's scree plot indicating the rank of the absorbance matrix (INDICES)											
Number of spectra measured, n_s		45	46	47	48	53	49	43	45	46	44
Number of wavelengths, n_w		187	187	187	188	187	188	187	187	187	187
Number of light-absorbing species, k^*		4	4	4	4	4	4	4	4	4	4
Residual standard deviation, $s_{k^*}(A)$ [mAU]		1.50	1.62	1.51	1.53	1.46	1.14	1.60	1.55	1.62	1.89
Estimates of dissociation constants in the searched protonation model											
pK_{a1} (s_1),	SQUAD84	2.12(02)	1.91(02)	1.79(01)	1.89(02)	2.01(02)	2.12(01)	1.95(02)	1.90(02)	2.04(01)	1.88(01)
$LH_4^{3+} = H^+ + LH_3^{2+}$	REACTLAB	2.12(01)	1.91(01)	1.78(01)	1.89(01)	2.00(01)	2.12(01)	1.94(01)	1.90(01)	2.04(01)	1.89(01)
pK_{a2} (s_2),	SQUAD84	4.18(02)	4.29(02)	4.16(01)	4.22(02)	4.18(02)	4.13(01)	4.17(02)	4.16(02)	4.07(01)	4.16(01)
$LH_3^{2+} = H^+ + LH_2^+$	REACTLAB	4.18(01)	4.29(01)	4.16(00)	4.22(01)	4.19(01)	4.13(00)	4.17(00)	4.16(00)	4.07(00)	4.16(01)
pK_{a3} (s_3),	SQUAD84	6.30(01)	6.27(01)	6.36(01)	6.16(01)	6.14(01)	6.29(01)	6.28(01)	6.24(01)	6.34(01)	6.22(01)
$LH_2^+ = H^+ + LH$	REACTLAB	6.30(01)	6.27(01)	6.36(01)	6.16(01)	6.20(01)	6.29(01)	6.28(01)	6.24(01)	6.34(01)	6.22(01)
Goodness-of-fit test with the statistical analysis of residuals											
Mean residual $E\|\bar{e}\|$	SQUAD84	1.13	1.22	1.13	1.15	1.11	1.08	1.18	1.15	1.19	1.38
[mAU]	REACTLAB	1.15	1.24	1.15	1.17	1.13	1.10	1.20	1.17	1.21	1.40
Standard deviation of	SQUAD84	1.50	1.62	1.51	1.53	1.46	1.45	1.60	1.55	1.62	1.89
residuals $s(\hat{e})$ [mAU]	REACTLAB	1.46	1.57	1.47	1.49	1.40	1.41	1.58	1.49	1.56	1.82
Sigma from ReactLab [mAU]	REACTLAB	1.48	1.59	1.48	1.51	1.44	1.43	1.56	1.52	1.59	1.85
Hamilton R-factor from SQUAD84 [%]	SQUAD84	0.49	0.44	0.39	0.47	0.53	0.38	0.38	0.40	0.44	0.46

ious authors such as the residual standard deviation RSD, the root mean error square RMS, the average error criterion AE, χ^2 criterion Chi2 and the standard deviation of eigenvalues g_k, ref. [42].

The set of spectra in Fig. 5 and the graph of the molar absorption coefficients in Figs. 4 show that there is a very small difference between the spectrum of L^- and LH_3^{+2} which is similar to the experimental noise $s_{inst}(A)$. Therefore, most modifications of the factor analysis in Fig. 3 determine the number of light-absorbing species equal to three, $k^* = 3$. However, the most sensitive method for determining the number of light-absorbing species is the graph of the eigenvalues $\log(g_k)$ which plotted against the index k led to correct $k^* = 4$. The number of light-absorbing species n_c is useful for solution equilibria study as it helps to establish the protonation model. This means that three dissociation constants will be preferred and four species LH_3^{2+}, LH_2^+, LH and L^- are supposed to be present in the equilibrium mixture. The coordinate of the break on the curve also enable to estimate the actual instrumental error $s_{inst}(A) = 1.1$ mAU of the experimental equipment used with the spectrophotometer CINTRA 5 (GBC, Australia).

Step 3: *Diagnostics for the search of the protonation model building and testing:* The hard modeling technique SQUAD84 and soft-modeling technique REACTLAB were used for the protonation model building. In both programs the same computational strategy was applied, *i. e.*, the *regression triplet* (criticism of data, model and method), *cf.* ref. [19,45]. The residuals-least-squares method *RSS* quantifies the sum of the deviations of the absorbances between the experimental and calculated spectra. The calculated spectrum is quantified as the sum of the contributions of all differently protonated species, when their concentrations being calculated for the estimated dissociation constants. In an iterative process, the molar absorption coefficients of these species are calculated. The suggested hypothesis of the protonated model forms the starting point for the iterative procedure. The search for the best hypothesis of the protonation model containing one, two or three dissociation constants is shown in Fig. 4, which presents the graphs of the molar absorption coefficients and the distribution diagrams of all the species from the three used hypotheses of the protonation model. The reliable criterion for the best hypothesis is based on the resulting goodness-of-fit test of the calculated spectra through the experimental absorbance matrix $s(A)$. The best fitness of spectra set was achieved for the hypothesis of four different protonated species LH_3^{2+}, LH_2^+, LH and L^-, although the L^- and LH_3^{2+} spectrum is almost the same.

Table 1 The estimates of the dissociation constants using two regression programs, *i.e.* SQUAD84 and REACTLAB were also compared, (Table 1). The mean residual $E|e|$ [mAU], the standard deviation of residuals $s(e)$ [mAU] and the Hamilton *R-factor* of relative fitness [%] in SQUAD84 generally showed that an excellent fit of the calculated spectra was achieved for the protonation model with three dissociation constants. REACTLAB seemed to offer the more reliable parameter estimates as it always reached a better curve fitting than the older program SQUAD84. The reliability of the regression parameter estimates may be tested using the following general diagnostics (Table 1 and Fig. 4) as has been previously elucidated in ref. [21]:

(a) *The physical meaning of parametric estimates.* In the left part of Fig. 4 the estimated molar absorptivities of all of the variously protonated species ε_L, ε_{LH}, ε_{LH2} and ε_{LH3} of lesinurad with regard to wavelength are shown. The curves of ε_L and ε_{LH3} seemed to be close and nearly the same.
(b) *The physical meaning of the species concentrations.* The distribution diagram (Fig. 4) shows the protonation equilibria of LH_3^{2+}, LH_2^+, LH and L^-. At pH 7 lesinurad has the species L^- and LH. Acidification of the species LH first creates the cation LH_2^+, and in a solution of pH 3 to pH 2 predominate cations LH_2^+ and LH_3^{2+}.
(c) *Goodness-of-fit test:* Although the statistical analysis of residuals [21] gives the most rigorous test of the goodness-of-fit, realistic empirical limits should be used. The statistical measures of all residuals e prove that the minimum of the elliptic hyperparaboloid *RSS* has been reached (Table 1): the mean residual $E|\bar{e}|$ [mAU] and the standard deviation of residuals $s(\hat{e})$ [mAU] always have sufficiently low values, lower than 2 mAU, which is less than 0.2% of the measured absorbance value proving in this way a good fitness. The good fitness achieved also is proven by small value of the Hamilton *R-factor* mostly less than 0.5%.

Step 4: *Reproducibility and choice of the wavelength range:* To examine the dependence of the proximity between the ionisable

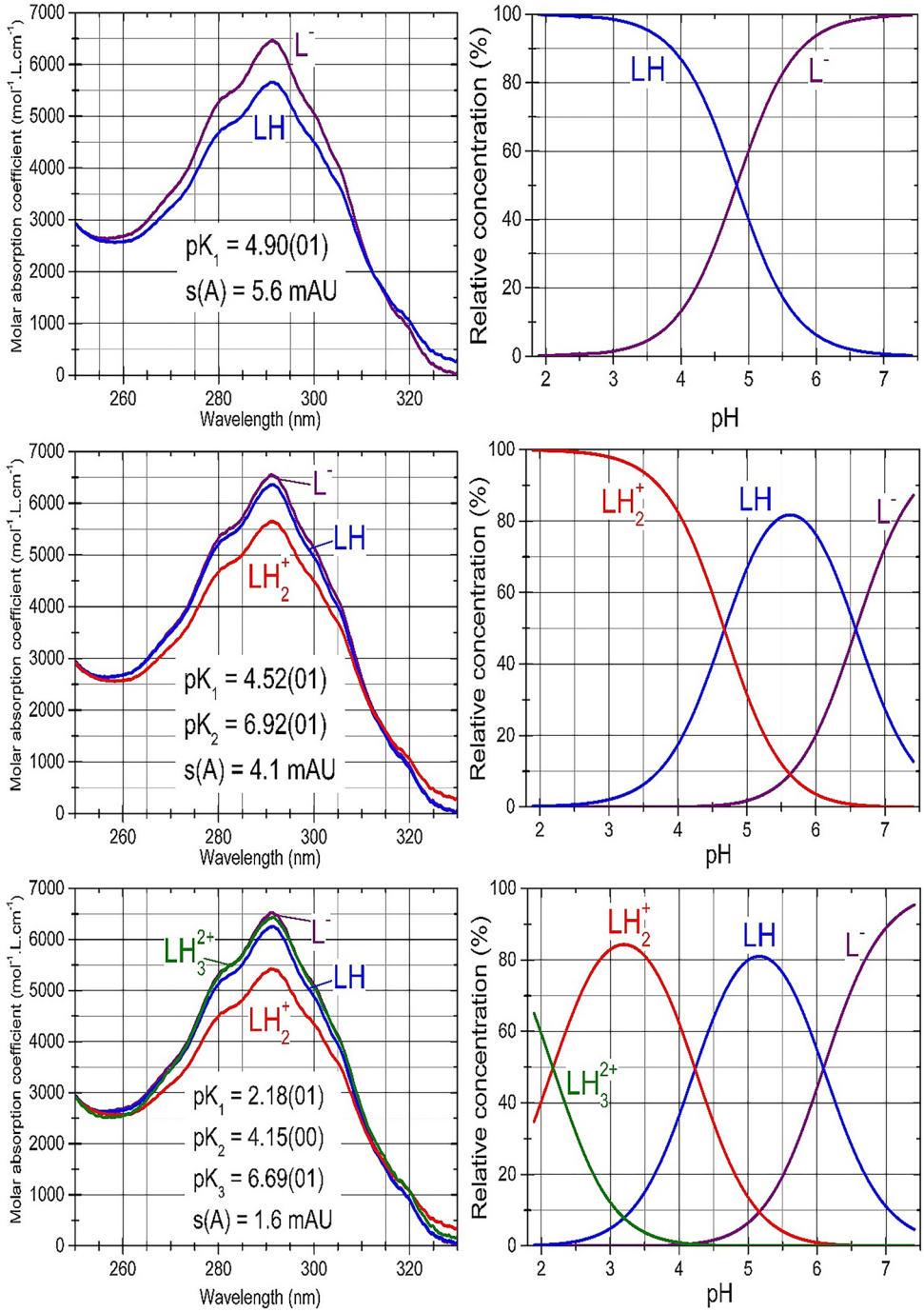

Fig. 4. Typical SQUAD84 working environment searching the best protonation model of lesinurad in the pH range from 2 to 8 for one, two and three dissociation constants pK_{a1}, pK_{a2}, pK_{a3} using 10^{-4} M lesinurad at $I = 0.0026$ at 25 °C. *Left:* The pure spectra profiles of molar absorptivities *vs.* wavelength (nm) for all of the variously protonated species of lesinurad. *Right:* The distribution diagram of the relative concentrations of all of the variously protonated species in dependence on pH, (REACTLAB, ORIGIN 9).

group and the chromophore, the spectral shift may not be strong enough to allow for a successful determination. It is important to select the wavelength range to assess the effect of the ionizable center on chromophore when changing pH. Three ranges of 250–330, 280–330 and 250–280 nm were selected for examination and the spectra were evaluated in these wavelength ranges. Fig. 5 shows the estimates of three dissociation constants including the achieved goodness-of-fit value $s(A)$, which serves as the criterion of certainty of the obtained estimates. The best fitness was achieved in the wavelength range 250–280 nm, although the dissociation constant estimates are nearly the same in all three ranges. The reproducibility of the dissociation constants treated with SQUAD84 and REACTLAB estimated from five reproduced measurements were found to be in good agreement at 25 °C and 37 °C (Table 1, Fig. 5).

Step 5: *Signal-to-noise ratio in analysis of small spectra changes*: In the spectrophotometric determination of pK_a of the lesinurad it is necessary to investigate whether the change in pH will cause a sufficient change in absorbance in the shape of a spectrum. Fig. 6a and b show that the spectral response to the chromophore in the lesinurad molecule is not large, so it was necessary to test whether it is possible to estimate the dissociation constants even from such

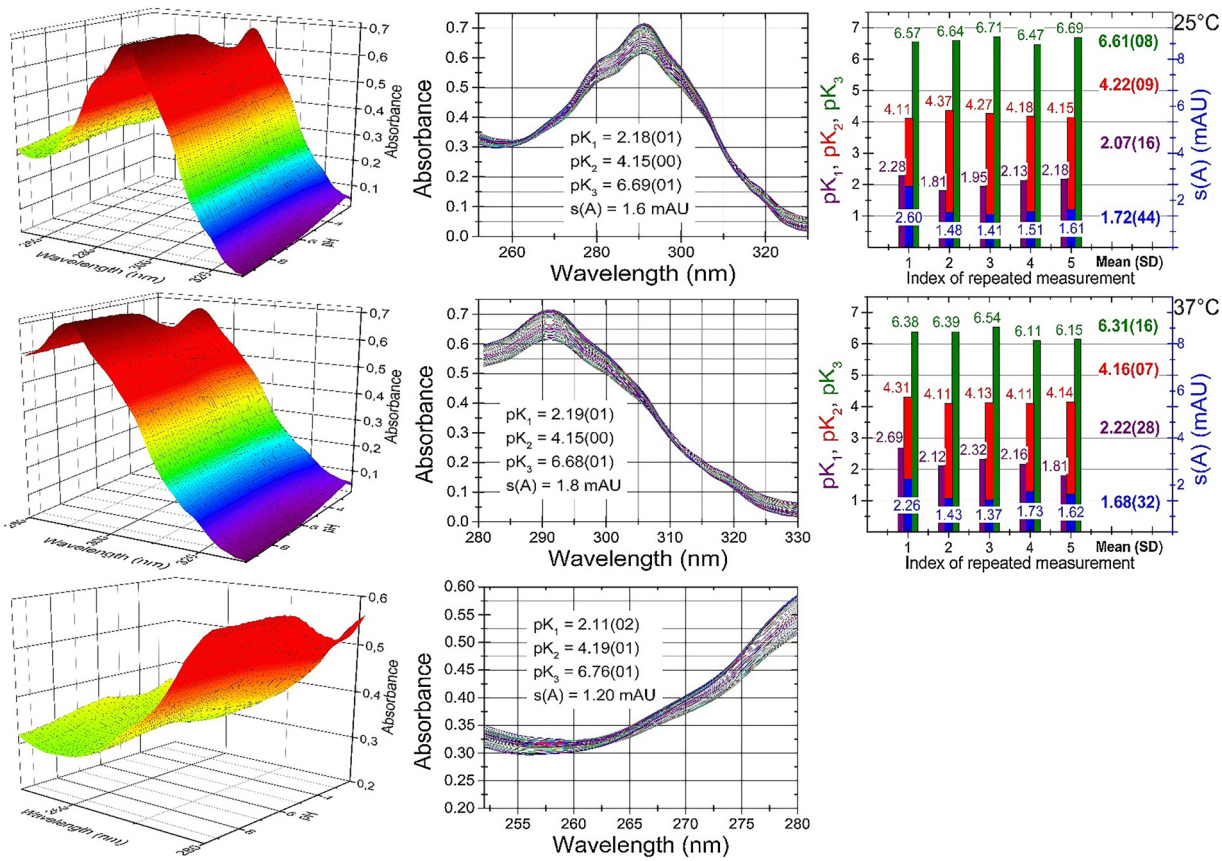

Fig. 5. *Left:* The plot of the 3D-absorbance-response-matrix for lesinurad representing the measured multiwavelength absorption spectra for lesinurad according to pH at 25 °C. Lesinurad in aqueous medium of phosphate buffer with adjusted ionic strength was titrated by HCl to pH 2 and after a subsequent retitration with KOH to pH 8 at 25 °C. *Middle:* The plot of the 2D-absorbance-response-matrix. *Right:* Reproducibility of the estimated dissociation constants evaluated in three absorption bands. The estimates of dissociation constants pK_{a1}, pK_{a2}, and pK_{a3} with their standard deviation in the last two digits are written. The goodness-of-fit is expressed as the standard deviation of absorbance after the regression was performed $s(A)$ [mAU], (REACTLAB, SQUAD84, ORIGIN 9).

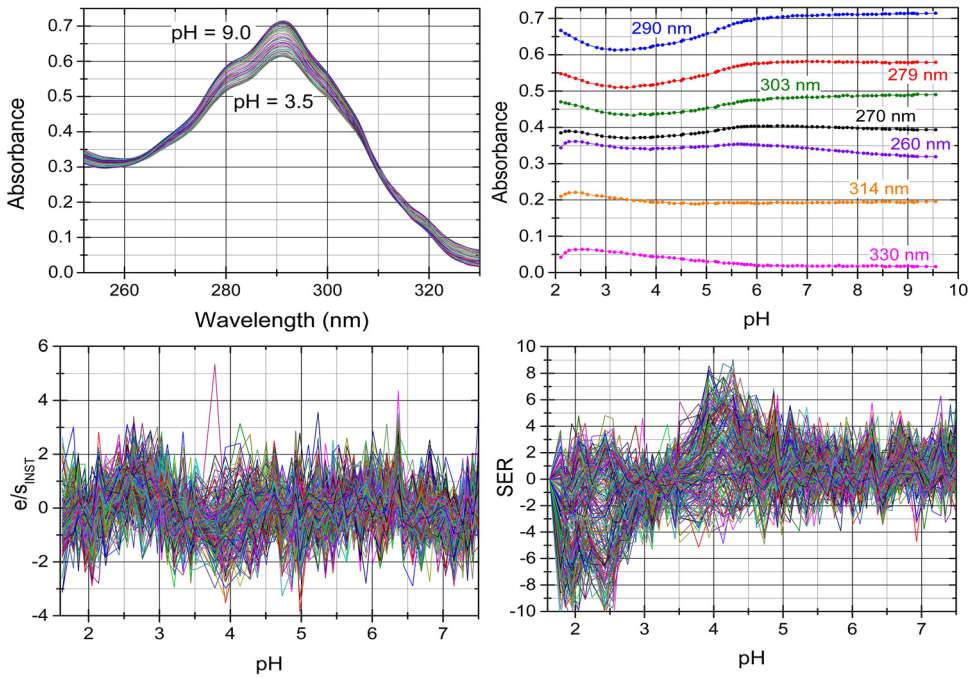

Fig. 6. (a) The plot of small absorbance changes in the lesinurad 2D-spectra set are within pH-titration, (b) Absorbance-pH curves are at selected wavelengths, (c) Residuals $\boldsymbol{e}$ [mAU] are divided by the instrumental standard deviation $e/s_{inst}(A)$ to test if the residuals $\boldsymbol{e}$ are of the same magnitude as the instrumental noise $s_{inst}(A)$, (d) The plot of small absorbance shift in the lesinurad spectrum within pH-titration when the value of the absorbance difference for the jth-wavelength of the ith-spectrum $\Delta_{ij} = A_{ij} - A_{i,acid}$ is divided by the instrumental standard deviation, leading to SER = $\Delta_{ij}/s_{inst}(A)$. This SER ratio is plotted on wavelength λ. Here $A_{i,acid}$ is the limiting spectrum of the acid form of the Lesinurad, (REACTLAB, ORIGIN 9).

small spectral changes. The change for the i-th spectrum and the j-th absorbance point of the spectrum were calculated as $\Delta_{ij} = A_{ij} - A_i$, and then divided with the instrumental standard deviation $s_{inst}(A)$, leading to the normalized spectra changes $SER = \Delta/s_{inst}(A)$. The A_i stands for the absorbance of acid form of lesinurad. It is necessary to investigate whether these small changes Δ in spectra are sufficiently larger than the size of the $s_{inst}(A)$. The *SER* changes in spectra is plotted versus the wavelength λ for all absorbance matrix elements (Fig. 6d) to show that even though these values are small they are still larger than the instrumental noise of the standardized residuals $e/s_{inst}(A)$ on Fig. 6c. While $e/s_{inst}(A)$ is here in the range (−2, +2), the changes in *SER* are in the range (−10, +10). Therefore, small variations in the spectra explain a larger degree of uncertainty in estimates of dissociation constants. The empirical rule should be kept in mind that if the *SER* is less than 10, the number of light-absorbing species n_c need not be correctly determined by the factor analysis in INDICES algorithm [43].

Step 6: *The deconvolution of spectra:* Decomposition of each experimental spectrum into spectra of the individual species proves whether the experimental design has been proposed efficient enough. In pH ranges where more components contribute significantly to the spectrum, several spectra should be measured. Such a spectrum provides sufficient information for a regression analysis which monitors at least two species in equilibrium where none of them represents a minor species. Fig. 7 presents six figures of the deconvolution of each measured spectrum into the absorption bands of the variously protonated lesinurad species. The consecutive deprotonation response in spectra of lesinurad is here demonstrated. At pH 1.925, the absorption band of the cation LH_3^{2+} is present in the equilibrium mixture accompanying the cation LH_2^+. From pH 2.237 to pH 4.035 the absorption band of cation LH_3^{2+} decreases as its concentration decreases and the absorption bands of cation LH_2^+ and neutral molecule LH increase. From pH 4.676 to pH 5.692, the LH concentration increases, the LH_2^+ concentration decreases to pH 6.513 and the LH_2^+ cation disappears and thus also its absorption band. Two absorption bands of LH and predominated anion L^- are present at pH 6.513.

4.2. pH-metric data analysis

The potentiometric titration of an acidified mixture of lesinurad with potassium hydroxide concerning the pH-metric data analysis was carried out at 25 °C and 37 °C for the adjusted value of ionic strength (Fig. 8). The initial tentative value of the dissociation constant of lesinurad studied was refined by the ESAB program.

Step 7: *Analysis of pH-metric data and Bjerrum's formation function:* Since lesinurad exhibits three dissociation constants, their numerical estimation is performed using computer-assisted nonlinear regression of the ESAB program. Regression analysis was employed by using a plateau of the middle part of the titration curve, which concerned acidified lesinurad titrated with potassium hydroxide, which is shown in the graph in Fig. 8. The estimates of the three dissociation constants pK_{a1}, pK_{a2} and pK_{a3} are plotted on the Bjerrum formation curves. At higher concentration than 2×10^{-4} M precipitate of lesinurad occurs which initially forms a slight opalescence.

Table 2 The ESAB residuals are defined as the difference between the experimental and calculated titrant volume $e_i = V_{exp,i} - V_{calc,i}$. The goodness-of-fit test is carried out with the statistical analysis of residuals. When further group parameters are also refined, the fit is improved. A quite sensitive criterion of the reliability of the dissociation constants estimated is the mean of absolute values of residuals $E|\bar{e}|$ [mL]. Comparing residuals with the instrumental noise, $s_{inst}(V)$, represented here by either $s_{inst}(V) = s(V) = 0.0001$ mL, an excellent fit is confirmed since the mean $E|\bar{e}|$ [mL] and also the residual standard deviation $s(\hat{e})$ [mL] are nearly the same, and are

Table 2
ESAB regression refinement of common and group parameters for a pH-metric titration of acidified lesinurad titrated with KOH: the estimated dissociation constants pK_{a1}, pK_{a2}, pK_{a3} of lesinurad when their standard deviations in last valid digits are in parentheses. The reliability of parameter estimation is proven with a goodness-of-fit statistics: the arithmetic mean of residuals $E(\hat{e})$ [mL], the mean of absolute value of residuals, $E|\hat{e}|$ [mL], the standard deviation of residuals $s(\hat{e})$ [mL], the residual skewness $g_1(\hat{e})$ and the residual kurtosis $g_2(\hat{e})$ proving a Gaussian distribution and Jarque-Berra normality test.

Temperature	25 °C					37 °C				
Ionic strength I_0 [mol/L]	0.0154	0.0305	0.0601	0.0858	0.0992	0.0154	0.0305	0.0601	0.0746	0.0863
Estimates of the group parameters H_0 and L_0 in the searched protonation model										
Number of points used n	44	44	29	38	32	33	31	42	35	41
$H_0 \times$ 1E+02 [mol/L]	3.26(00)	3.23(00)	3.11(00)	3.12(00)	3.06(00)	3.21(00)	3.25(00)	3.15(00)	3.04(00)	2.98(00)
$L_0 \times$ 1E+04 [mol/L]	1.62(02)	1.89(02)	3.58(01)	2.13(02)	3.13(04)	1.30(04)	1.27(02)	1.52(03)	1.55(04)	1.86(05)
Estimates of the common parameters *i.e.* dissociation constants in the searched protonation model										
$pK_{a1}(s_1)$	2.39(05)	2.37(07)	2.22(05)	2.39(07)	2.33(06)	2.10(04)	2.09(05)	2.08(06)	2.10(06)	2.12(07)
$pK_{a2}(s_2)$	3.54(02)	3.57(01)	3.55(04)	3.66(01)	3.57(02)	3.36(06)	3.40(07)	3.44(04)	3.51(05)	3.40(06)
$pK_{a3}(s_3)$	6.15(02)	6.16(01)	6.13(03)	6.15(01)	6.13(02)	6.02(05)	6.01(05)	6.06(03)	6.00(04)	5.99(05)
Goodness-of-fit test with the statistical analysis of residuals										
Arithmetic mean of residuals $E(\hat{e})$, [mL]	-2.27E-06	-4.32E-05	6.89E-05	4.73E-05	-7.69E-05	1.52E-05	5.71E-05	4.86E-05	-2.94E-06	1.71E-05
Mean of absolute value of residuals, $E|\hat{e}|$, [mL]	0.00015	0.00012	0.00059	0.00015	0.00030	0.00019	0.00014	0.00026	0.00026	0.00037
Residual standard deviation, $s(\hat{e})$, [mL]	0.00021	0.00016	0.00067	0.00018	0.00035	0.00028	0.00019	0.00035	0.00033	0.00051
Residual skewness $g_1(\hat{e})$	−0.14	0.00	−0.08	0.33	−0.06	−0.92	−0.23	−0.10	0.52	−0.72
Residual kurtosis $g_2(\hat{e})$	2.90	3.43	1.61	2.35	1.95	3.42	3.14	3.52	2.91	4.72
Jarque-Berra test of residuals normality: p, Normality is	0.862, Accepted	0.975, Accepted	0.943, Accepted	0.582, Accepted	0.955, Accepted	0.092, Accepted	0.783, Accepted	0.925, Accepted	0.343, Accepted	0.139, Accepted

Common parameters refined: pK_{a1}, pK_{a2}, pK_{a3}. ***Group parameters refined:*** H_0, L_0. ***Constants:*** $H_T = 0.9304$ mol/L, $t = 25.0$ °C, $pK_w = 13.9799$, $s(V) = s_{inst}(y) = 0.0001$ mL, I_0 adjusted (in vessel), $I_T = 0.9303$ (in burette KOH) or 1.0618 (in burette HCl).

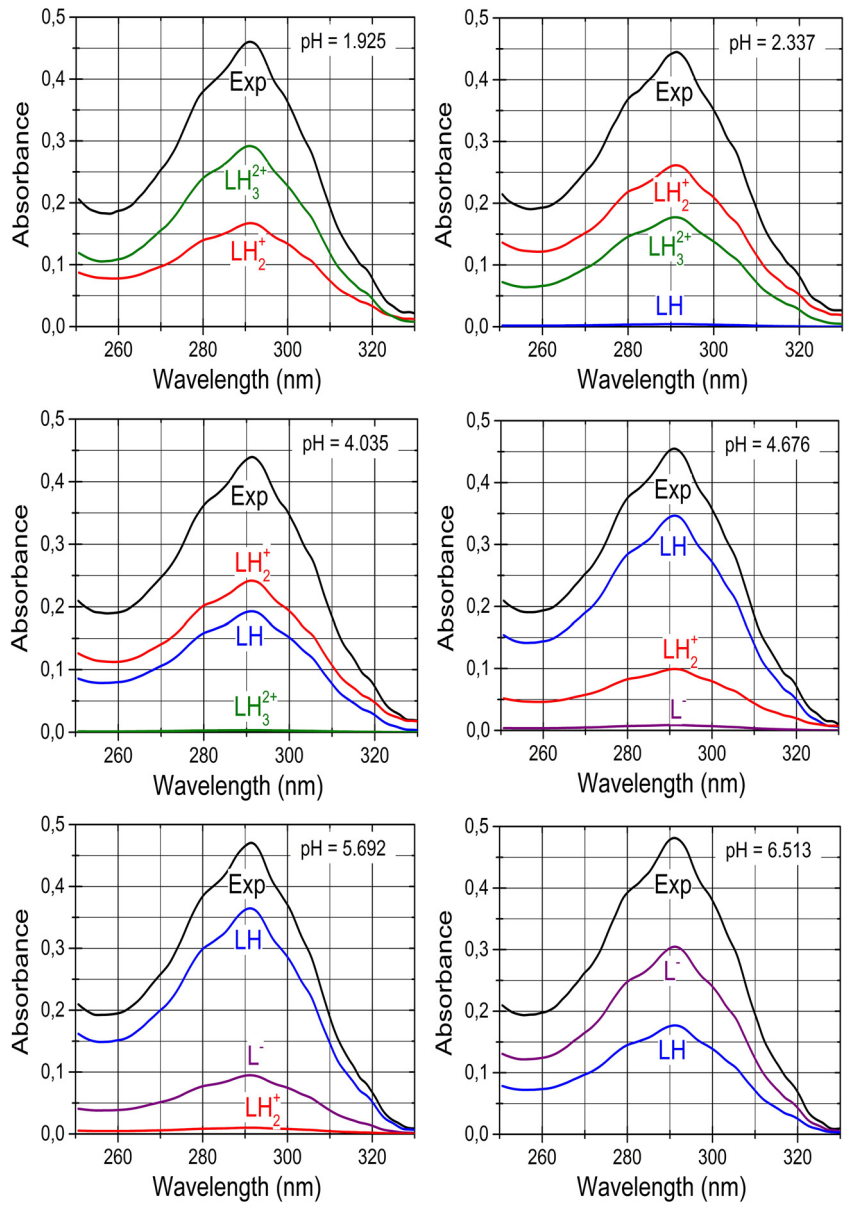

Fig. 7. Deconvolution of the each experimental spectrum of 10^{-4} M lesinurad at $I = 0.0026$ at 25 °C into spectra of the individual variously protonated species L^-, LH, LH_2^+, LH_3^{2+} in mixture for pH 1.925, 2.337, 4.035, 4.676, 5.692, 6.513 using SQUAD84.

lower than the experimental noise $s_{inst}(y)$. Here, $E|\bar{e}| = 0.0001$ mL and $s(\hat{e}) = 0.0001$ mL are similar and both are the same as the microburette error $s(V) = 0.0001$ mL. All residuals oscillate between the lower −0.0001 mL and upper limit 0.0001 mL of Hoaglin's inner bounds and therefore no outlying residuals were indicated outside these bounds (*cf.* page 80 in ref. [46]). The estimates of the dissociation constants estimated by ESAB are reliable (Table 2). The curve-fittness is improved using the refinement of the group parameter L_0, the actual concentration of the titrated drug lesinurad.

Step 8: *Thermodynamic dissociation constants:* Applying a Debye-Hückel equation to the data of Table 1 and 2 the unknown parameter pK^T_a has been estimated at two temperatures 25 °C and 37 °C. Because of the narrow range and small values of ionic strength the ion-size parameter $\mathring{a}$ and the salting-out coefficient C could not be estimated. Fig. 9 brings the extrapolation of the mixed dissociation constants to the zero value of ionic strength according to the limited Debye-Hückel law for the protonation model of three dissociation constants at temperatures 25 °C and 37 °C: $pK^T_{a1} = 2.09$, $pK^T_{a2} = 4.25$, $pK^T_{a3} = 6.58$ at 25 °C and $pK^T_{a1} = 1.96$, $pK^T_{a2} = 4.16$, $pK^T_{a3} = 6.32$ at 37 °C (spectrophotometricaly) and $pK^T_{a1} = 2.39$, $pK^T_{a2} = 3.47$, $pK^T_{a3} = 6.17$ at 25 °C and $pK^T_{a1} = 2.08$, $pK^T_{a2} = 3.29$, $pK^T_{a3} = 6.03$ at 37 °C (potenciometricaly).

Step 9: *Determination of enthalpy and entropy change:* The enthalpy change (ΔH^0) for the dissociation process was calculated using the van't Hoff equation $d\ln K/dT = \Delta H^0/RT^2$. From the free-energy change ΔG^0 and ΔH^0 values, the entropy ΔS^0 could be calculated: $\Delta G^0 = -RT \ln K$ and $\Delta S^0 = (\Delta H^0 - \Delta G^0)/T$, where R (ideal gas constant) = 8.314 J K^{-1} mol^{-1}, K is the thermodynamic dissociation constant, and T is the absolute temperature. Thermodynamic parameters ΔH^0 and ΔG^0 have been determined from the temperature variation of dissociation constants using van't Hoff's equation. The values of enthalpy $\Delta H^0(pK_{a1}) = 19.19$ kJ mol^{-1}, $\Delta H^0(pK_{a2}) = 13.29$ kJ mol^{-1}, $\Delta H^0(pK_{a3}) = 38.39$ kJ mol^{-1}, show the dissociation process is endothermic. The positive values of $\Delta G^0(pK_{a1}) = 11.93$ kJ mol^{-1}, $\Delta G^0(pK_{a2}) = 24.26$ kJ mol^{-1}, $\Delta G^0(pK_{a3}) = 37.56$ kJ mol^{-1} at 25 °C indicate that the dissociation process of pK_{a2} is not spontaneous, which was

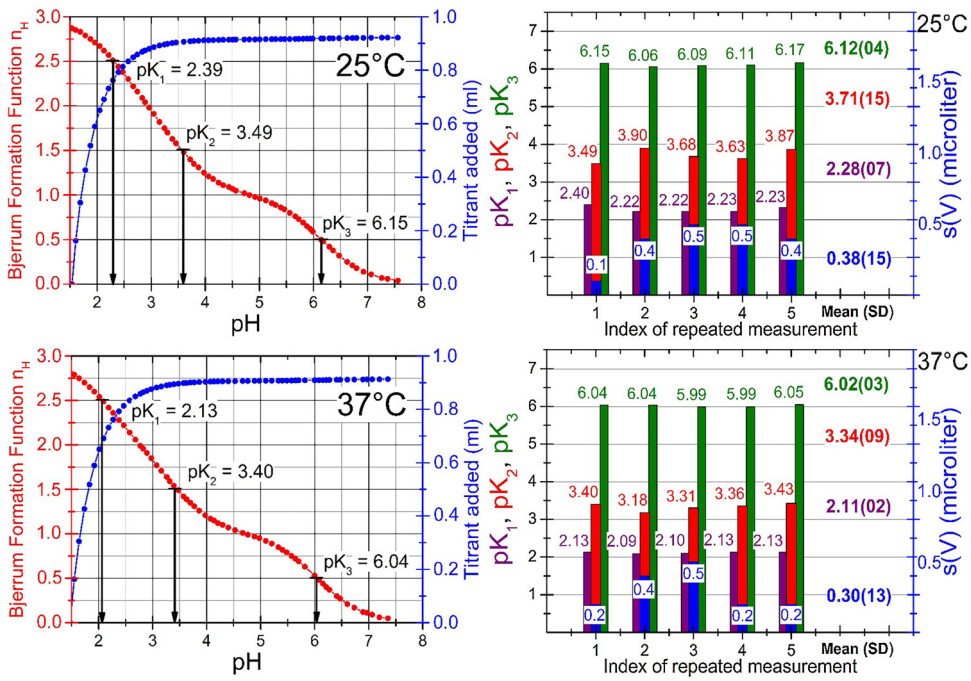

Fig. 8. The search for the protonation model analysing the potentiometric titration curve of acidified lesinurad and titrated with KOH and plotted with the Bjerrum protonation function indicating three pK_a values. Dissociation constants are estimated with ESAB at 25 °C and 37 °C (ESAB, ORIGIN).

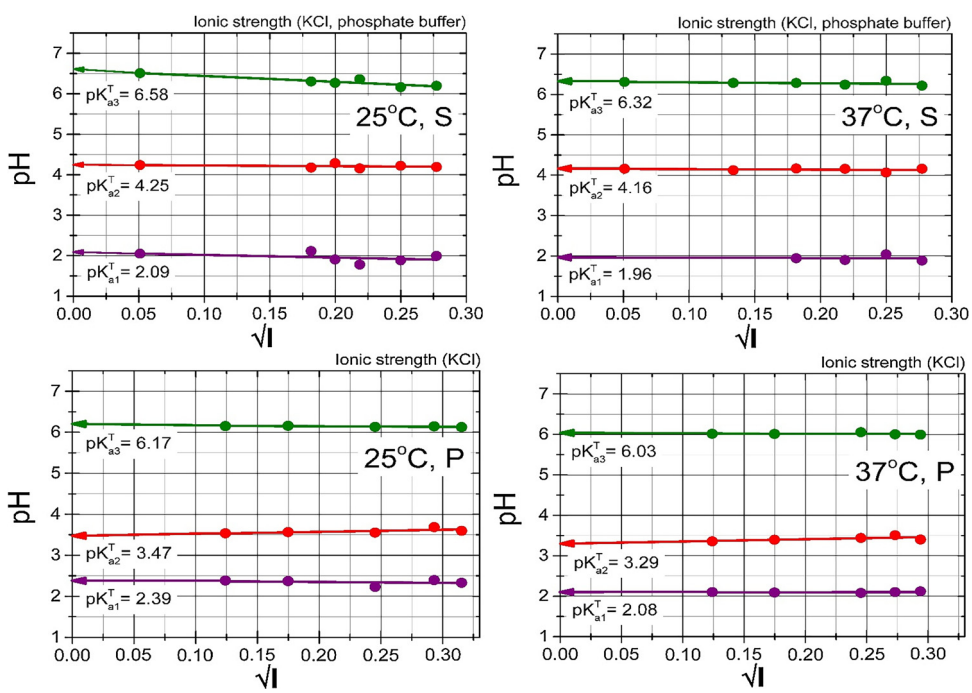

Fig. 9. Dependence of the mixed dissociation constants of lesinurad on the square root of the ionic strength for three dissociation constants leading to the thermodynamic dissociation constant pK^T_a at 25 °C *(left)* and 37 °C *(right)* using UV-metric technique *(S, Upper)* and pH-metric *(P, Lower)*.

confirmed by its value of entropy $\Delta S^0(pK_{a1}) = 24.37\,J\,mol^{-1}$, $\Delta S^0(pK_{a2}) = -36.79\,J\,mol^{-1}$, $\Delta S^0(pK_{a3}) = 2.79\,J\,mol^{-1}$.

5. Discussion

Both REACTLAB and SQUAD84 programs for spectra analysis produce for the spectrophotometric concentration 10^{-4} M of lesinurad the same estimates of all three dissociation constants which exhibit identical goodness-of-fit tests. The ESAB program minimizing residuals $e_i = V_{exp,i} - V_{calc,i}$ reaches 0.1 or 0.2 microlitres, thus proving an excellent fit. It may be concluded that the reliability of the dissociation constants of lesinurad was proven though the *group parameters* L_0, H_T were ill-conditioned in the model. The goodness-of-fit proved sufficient reliability of the parameter estimates for three dissociation constants of the lesinurad at 25 °C and 37 °C. The discrepancy of the found experimental pK and its predicted values might be caused by the unclear resonance structure of the heterocyclic core, and, consequently, different electron distribution, which can further lead to different pre-

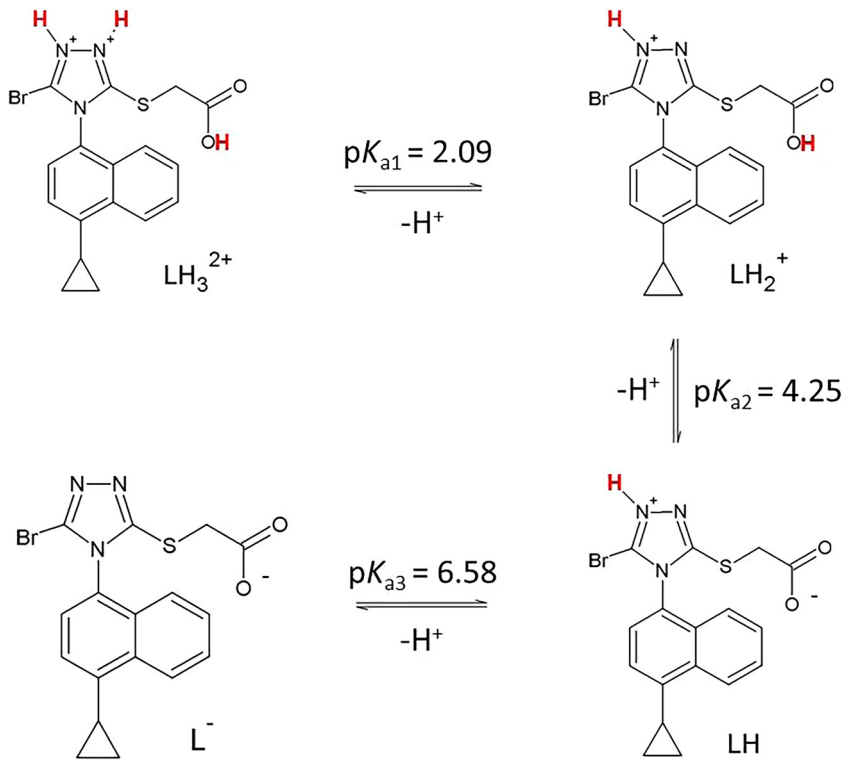

Scheme 1. Protonation scheme of the lesinurad.

dicted values according to the proposed structure. In such cases, the prediction programs MARVIN and ACD/Percepta may fail, and experimental laboratory determination is needed. As both potentiometric and spectrophotometric results are similar regarding the goodness-of-fit tests, the conclusion can be drawn that the obtained experimental results are reliable and that they show the real dissociation of the substance.

6. Conclusion

1) Spectrophotometric and potentiometric pH-titration allowed the measurement of three dissociation constants of lesinurad (Scheme 1). Chromophores of lesinurad exhibit small changes in the UV/VIS-spectrum at the solution pH change and therefore a determination of the dissociation constants is subject to greater uncertainty than in case of a potentiometric determination. Therefore, the more reliable estimate of dissociation constants are those obtained with potentiometric determination.
2) The sparingly soluble anion L^- of lesinurad capable of protonation to form the still soluble three species LH, LH_2^+, LH_3^{2+} occurs in pure water. The graph of molar absorption coefficients of variously protonated species according to wavelength shows that the spectrum of species L^- and LH_3^{2+} are nearly the same in colour.
3) We have proven that in the range of pH 2–8 three dissociation constants can be reliably estimated from the spectra when concentration of lesinurad is about 10^{-4} M. Although the somewhat less affected pH changes in the chromophore, three thermodynamic dissociation constants can be reliably determined with SQUAD84 and REACTLAB reaching the similar values with both programs, $pK^T_{a1} = 2.09$, $pK^T_{a2} = 4.25$, $pK^T_{a3} = 6.58$ at 25 °C and $pK^T_{a1} = 1.96$, $pK^T_{a2} = 4.16$, $pK^T_{a3} = 6.32$ at 37 °C (Fig. 9).
4) Three thermodynamic dissociation constants of lesinurad in a potentiometric concentration of 3×10^{-4} M were determined by the regression analysis of potentiometric titration curves using ESAB, $pK^T_{a1} = 2.39$, $pK^T_{a2} = 3.47$, $pK^T_{a3} = 6.17$ at 25 °C and $pK^T_{a1} = 2.08$, $pK^T_{a2} = 3.29$, $pK^T_{a3} = 6.03$ at 37 °C (Fig. 9).
5) Prediction of the dissociation constants of lesinurad was performed using the MARVIN program to specify protonation locations and using the ACD/Percepta program. In comparing two predictive and two experimental techniques, it may be concluded that the prediction programs sometimes vary in estimating pK_a.
6) Thermodynamic parameters ΔH^0 and ΔG^0 have been determined from the temperature variation of dissociation constants estimated from spectra analysis using the van't Hoff's equation. The values of enthalpy $\Delta H^0(pK_{a1}) = 19.19\ kJ\ mol^{-1}$, $\Delta H^0(pK_{a2}) = 13.29\ kJ\ mol^{-1}$, $\Delta H^0(pK_{a3}) = 38.39\ kJ\ mol^{-1}$, show the dissociation process is endothermic. The positive values of $\Delta G^0(pK_{a1}) = 11.93\ kJ\ mol^{-1}$, $\Delta G^0(pK_{a2}) = 24.26\ kJ\ mol^{-1}$, $\Delta G^0(pK_{a3}) = 37.56\ kJ\ mol^{-1}$ at 25 °C indicate that the dissociation process of pK_{a2} is not spontaneous, which was confirmed by its negative value of entropy $\Delta S^0(pK_{a1}) = 24.37\ J\ mol^{-1}$, $\Delta S^0(pK_{a2}) = -36.79\ J\ mol^{-1}$, $\Delta S^0(pK_{a3}) = 2.79\ J\ mol^{-1}$.

References

[1] F. Rees, M. Hui, M. Doherty, Optimizing current treatment of gout, Nat. Rev. Rheumatol. 10 (5) (2014) 271–283.
[2] M.D. Sanchez-Nino, B. Zheng-Lin, L. Valino-Rivas, A.B. Sanz, A.M. Ramos, J. Luno, M. Goicoechea, A. Ortiz, Lesinurad: what the nephrologist should know, Clin. Kidney J. 10 (2017) 679–687.
[3] N. Schlesinger, Difficult-to-Treat gout arthritis, Drugs 71 (2011) 26.
[4] Y. Garg, V. Gawri, R. Gore, R.S. Garg, A. Kumar, Lesinurad, a novel uricosuric drug for allopurinol-refractory gout patients, J. Clin. Diagnostic Res. 12 (2018) 5.
[5] A. Gupta, P.K. Sharma, A.K. Misra, S. Singh, Lesinurad A significant advancement or just another addition to existing therapies of gout? J. Pharmacol. Pharmacol. 7 (2016) 155–158.
[6] B. Pathare, V. Tambe, V. Patil, A review on various analytical methods used in determination of dissociation constant, Int. J. Pharm. Pharm. Sci. 6 (2014) 26–34.
[7] J. Reijenga, A.V. Hoof, A.V. Loon, B. Teunissen, Development of Methods for the Determination of pKa Values, Anal. Chem. Insights 8 (2013) 53–71.

[8] J.A. Hernández, A.R. Hernández, E.M.C. Urbina, I.M.D.L.G. Rodríguez, M.V. Manzanares, L.F. Medina-Vallejo, New chemometric strategies in the spectrophotometric determination of pKa, Chem. Eur. J. 5 (2014) 1–5.
[9] T.H. Shayesteh, M. Radmehr, F. Khajavi, R. Mahjub, Application of chemometrics in determination of the acid dissociation constants (pK(a)) of several benzodiazepine derivatives as poorly soluble drugs in the presence of ionic surfactants, Eur. J. Pharm. Sci. 69 (2015) 44–50.
[10] M.M. Pandey, A. Jaipal, A. Kumar, R. Malik, S.Y. Charde, Determination of pK(a) of felodipine using UV-Visible spectroscopy, Spectrochim. Acta A 115 (2013) 887–890.
[11] D.T. Manallack, The pK(a) distribution of drugs: application to drug discovery, Perspect. Med. Chem. 1 (2007) 25–38.
[12] F. Milletti, L. Storchi, G. Sforna, G. Cruciani, New and original pKa prediction method using grid molecular interaction fields, J. Chem. Inf. Model. 47 (2007) 2172–2181.
[13] L. Settimo, K. Bellman, R.A. Knegtel, Comparison of the accuracy of experimental and predicted pKa values of basic and acidic compounds, Pharm. Res. 31 (2014) 1082–1095.
[14] K.Y. Tam, K. Takacs-Novak, Multiwavelength spectrophotometric determination of acid dissociation constants: a validation study, Anal. Chim. Acta 434 (2001) 157–167.
[15] R.I. Allen, K.J. Box, J.E.A. Comer, C. Peake, K.Y. Tam, Multiwavelength spectrophotometric determination of acid dissociation constants of ionizable drugs, J. Pharm. Biomed. Anal. 17 (1998) 699–712.
[16] F.R. Hartley, C. Burgess, R.M. Alcock, Solution Equilibria, Ellis Horwood, Chichester, 1980.
[17] D.J. Leggett, W.A.E. McBryde, General computer program for the computation of stability constants from absorbance data, Anal. Chem. 47 (1975) 1065–1070.
[18] J.J. Kankare, Computation of equilibrium constants for multicomponent systems from spectrophotometric data, Anal. Chem. 42 (1970) 1322–1326.
[19] M. Meloun, Z. Ferenčíková, M. Javůrek, Reliability of dissociation constants and resolution capability of SQUAD(84) and SPECFIT/32 in the regression of multiwavelength spectrophotometric pH-titration data, Spectrochim. Acta. A. Mol. Biomol. Spectrosc. 86 (2012) 305–314.
[20] M. Meloun, V. Nečasová, M. Javůrek, T. Pekárek, The dissociation constants of the cytostatic bosutinib by nonlinear least-squares regression of multiwavelength spectrophotometric and potentiometric pH-titration data, J. Pharm. Biomed. Anal. 120 (2016) 158–167.
[21] M. Meloun, S. Bordovská, T. Syrový, A. Vrána, Tutorial on a chemical model building by least-squares non-linear regression of multiwavelength spectrophotometric pH-titration data, Anal. Chim. Acta 580 (2006) 107–121.
[22] M. Meloun, S. Bordovská, A. Vrána, The thermodynamic dissociation constants of the anticancer drugs camptothecine 7-ethyl-10-hydroxycamptothecine, 10-hydroxycamptothecine and 7-ethylcamptothecine by the least-squares nonlinear regression of multiwavelength spectrophotometric pH-titration data, Anal. Chim. Acta 584 (2007) 419–432.
[23] M. Meloun, L. Pilarova, T. Pekarek, M. Javurek, Overlapping pK(a) of the multiprotic hemostyptic eltrombopag using UV–vis multiwavelength spectroscopy and potentiometry, J. Solution Chem. 46 (2017) 2014–2037.
[24] M. Maeder, P. King, Analysis of Chemical Processes, Determination of the Reaction Mechanism and Fitting of Equilibrium and/or Rate Constants, in K. Varmuza (Ed) Chemometrics in Practical Applications, 2012, pp. 41–62, ISBN: 978-953-51-0438-4, InTech, Available from: http://www.intechopen.com/books/chemometrics-in-practical-applications/analysis-of-chemical-processesdetermination-of-the-reaction-mechanism-and-fitting-of-equilibrium-an.
[25] D.J. Leggett, S.L. Kelly, L.R. Shiue, Y.T. Wu, D. Chang, K.M. Kadish, A computational approach to the spectrophotometric determination of stability constants-II. Application to metalloporphyrin-axial ligand interactions in non-aqueous solvents, Talanta 30 (1983) 579–586.
[26] C. De Stefano, P. Princi, C. Rigano, S. Sammartano, Computer analysis of equilibrium data in solution ESAB2 M: an improved version of the ESAB program, Anal. Chim. 77 (1987) 643–675.
[27] P. Gans, A. Sabatini, A. Vacca, Investigation of equilibria in solution. Determination of equilibrium constants with the HYPERQUAD suite of programs, Talanta 43 (1996) 1739–1753.
[28] P. Gans, A. Sabatini, A. Vacca, Hyperquad computer-program suite, Abstr. Pap. Am. Chem. S 219 (2000), U763–U763.
[29] A.R. Ribeiro, T.C. Schmidt, Determination of acid dissociation constants (pK(a)) of. cephalosporin antibiotics: computational and experimental approaches, Chemosphere 169 (2017) 524–533.
[30] ACD/Labs pKa Predictor 3.0, in: A.C.D. Inc. (Ed.) Toronto, Canada, 2007.
[31] G.T. Balogh, B. Gyarmati, B. Nagy, L. Molnar, G.M. Keseru, Comparative evaluation of in silico pK(a) prediction tools on the gold standard dataset, Qsar. Comb. Sci. 28 (2009) 1148–1155.
[32] G.T. Balogh, A. Tarcsay, G.M. Keseru, Comparative evaluation of pK(a) prediction tools on a drug discovery dataset, J. Pharm. Biomed. Anal. 67-68 (2012) 63–70.
[33] V. Evagelou, A. Tsantili-Kakoulidou, M. Koupparis, Determination of the dissociation constants of the cephalosporins cefepime and cefpirome using UV spectrometry and pH potentiometry, J. Pharm. Biomed. Anal. 31 (2003) 1119–1128.
[34] C.Z. Liao, M.C. Nicklaus, Comparison of nine programs predicting pK(a) values of pharmaceutical substances, J. Chem. Inf. Model. 49 (2009) 2801–2812.
[35] G. Roda, C. Dallanoce, G. Grazioso, V. Liberti, M. De Amici, Determination of acid dissociation constants of compounds active at neuronal nicotinic acetylcholine receptors by means of electrophoretic and potentiometric techniques, Anal. Sci. 26 (2010) 51–54.
[36] J. Bezencon, M.B. Wittwer, B. Cutting, M. Smiesko, B. Wagner, M. Kansy, B. Ernst, pK(a) determination by H-1 NMR spectroscopy – An old methodology revisited, J. Pharm. Biomed. Anal. 93 (2014) 147–155.
[37] N.T. Hansen, I. Kouskoumvekaki, F.S. Jorgensen, S. Brunak, S.O. Jonsdottir, Prediction of pH-dependent aqueous solubility of druglike molecules, J. Chem. Inf. Model. 46 (2006) 2601–2609.
[38] J. Manchester, G. Walkup, O. Rivin, Z.P. You, Evaluation of pK(a) estimation methods on 211 drug like compounds, J. Chem. Inf. Model. 50 (2010) 565–571.
[39] T. ten Brink, T.E. Exner, pK(a) based protonation states and microspecies for protein-ligand docking, J Comput. Aid. Mol. Des. 24 (2010) 935–942.
[40] M. Meloun, T. Syrový, S. Bordovská, A. Vrána, Reliability and uncertainty in the estimation of pK (a) by least squares nonlinear regression analysis of multiwavelength spectrophotometric pH titration data, Anal. Bioanal. Chem. 387 (2007) 941–955.
[41] M. Meloun, J. Havel, E. Högfeldt, Computation of Solution Equilibria: A Guide to Methods in Potentiometry, Extraction, and Spectrophotometry, Ellis Horwood, Chichester, England, 1988.
[42] C. Rigano, M. Grasso, S. Sammartano, Computer-analysis of equilibrium data in solution – a compact least-squares computer-program for acid-base titrations, Anal. Chim. 74 (1984), 537–532.
[43] M. Meloun, J. Čapek, P. Mikšík, R.G. Brereton, Critical comparison of methods predicting the number of components in spectroscopic data, Anal. Chim. Acta 423 (2000) 51–68.
[44] ORIGIN, OriginLab Corporation, One Roundhouse Plaza, Suite 303, Northampton, MA 01060, USA.
[45] M. Meloun, J. Militký, M. Forina, Chemometrics for Analytical Chemistry, Volume 2: PC- Aided Regression and Related Methods, Ellis Horwood, Chichester, 1994.
[46] M. Meloun, J. Militký, M. Forina, Chemometrics for Analytical Chemistry, Volume 1: PC-Aided Statistical Data Analysis, Ellis Horwood, Chichester, 1992.